Equilibrium Unfolding of Yeast Phosphoglycerate Kinase and Its Mutants Lacking One or Both Native Tryptophans: A Circular Dichroism and Steady-State and Time-Resolved Fluorescence Study†

Barbara K. Szpikowska,‡ Joseph M. Beechem,§ Mark A. Sherman,‡ and Maria T. Mas*,‡

Division of Biology, Physical Biochemistry Section, Beckman Research Institute of the City of Hope, Duarte, California 91010, and Department of Molecular Physiology and Biophysics, Vanderbilt University, Nashville, Tennessee 37232

Received July 30, 1993; Revised Manuscript Received January 4, 1994®

ABSTRACT: Yeast 3-phosphoglycerate kinase contains two tryptophans, both situated in the carboxy-terminal domain, and seven tyrosines, five in the amino-terminal domain, one in the domain–domain interface, and one in the carboxy-terminal domain. Site-specific mutagenesis has been used to construct two single-tryptophan mutants and one no-tryptophan mutant by replacing one or both native tryptophans, W308 and W333, with phenylalanines. The mutations have been shown to have a relatively small effect on the overall structure and enzymatic properties of the mutants. Both tryptophans are quenched in the folded state. The steady-state emission spectra and tryptophan quantum yields are the same in the single-tryptophan mutants and in the wild-type protein. Large changes in the tryptophan emission maxima and steady-state emission intensities are observed upon unfolding. Far-UV circular dichroism and steady-state as well as time-resolved fluorescence spectroscopy have been used to monitor the equilibrium unfolding transitions of these mutants and wild-type PGK. For each protein, the transitions followed by CD and steady-state fluorescence are nearly coincident, suggesting that the structural changes monitored by local fluorescence probes and ellipticity changes, which are sensitive to the changes in the overall structure, report a single cooperative transition, consistent with a two-state unfolding mechanism. Both tryptophans have three lifetimes, which follow a similar pattern as a function of denaturant concentration. The amplitude terms associated with the two longer lifetimes increase with unfolding while the short lifetime amplitude decreases. It thus appears that these population amplitudes represent markers for the unfolded and folded states, respectively. The transition midpoints calculated from the analysis of each amplitude term are identical with those determined from the steady-state total intensity changes. In contrast, those determined from the lifetime changes and from the preexponential associated with the long correlation time appear to precede the transitions followed by steady-state intensity changes and CD. The time-resolved anisotropy decays associated with WT, W308, and W333 are distinct in the folded proteins and become essentially identical in the unfolded state.

Native tyrosines and tryptophans have been used extensively as sensitive intrinsic fluorescence probes of protein conformational changes. Since most proteins contain multiple tryptophans and tyrosines, it is usually difficult to interpret the observed spectral changes in terms of specific structural changes. Recently, genetic engineering has been exploited to resolve fluorescence properties of multi-tryptophan-containing proteins (Royer et al., 1990; Harris & Hudson, 1990; Axelsen et al., 1991; Atkins et al., 1991; Loewenthal et al., 1991; Willaert et al., 1992) and to produce single-tryptophan mutants for folding studies (Smith et al., 1991; Staniforth et al., 1993).

Yeast phosphoglycerate kinase (PGK[1]) contains two tryptophans, W308 and W333, both situated in the carboxy-terminal domain. In addition, there are seven tyrosines, five of which are situated in the amino-terminal domain, one in the interdomain hinge region, and one in the carboxy-terminal domain near the domain–domain interface (Figure 1). According to the crystallographically determined structure of yeast PGK (Watson et al., 1982), W308 is situated on the surface and is surrounded by several charged amino acid residues. In contrast, W333 is buried in a hydrophobic environment.

Unusual fluorescence properties have been reported for yeast PGK by Nojima et al. (1976, 1977). These authors reported an unusually large contribution of the tyrosyl fluorescence at excitation wavelength 280 nm to the fluorescence emission spectrum and a very low quantum yield of tryptophanyl fluorescence. A significant increase in the tryptophanyl quantum yield upon unfolding has led to the suggestion that at least one or possibly both of the tryptophans are quenched in the native form of PGK (Nojima et al., 1976). Time-resolved fluorescence studies (Privat et al., 1980; Wasylewski & Eftink, 1987) revealed that tryptophanyl fluorescence decay in yeast PGK can be resolved into three components and

† This research was supported in part by National Institutes of Health Grants GM33715 and GM41360 to M.T.M. Support by Cancer Center Support Grant CA33572 for the Computer Graphics Facility (M.T.M.) is also acknowledged. J.M.B. gratefully acknowledges support from the Lucille P. Markey Foundation and NIH Grant GM45990.

* Author to whom correspondence should be addressed.
‡ Beckman Research Institute of the City of Hope.
§ Vanderbilt University.

® Abstract published in *Advance ACS Abstracts,* February 1, 1994.

[1] Abbreviations: PGK, 3-phosphoglycerate kinase; WT, wild type; W308 PGK, PGK mutant with a single native tryptophan at position 308 and a phenylalanine substituted for tryptophan 333; W333 PGK, PGK mutant with a single native tryptophan at position 333 and a phenylalanine substituted for tryptophan 308; W⁻ PGK, a no-tryptophan mutant in which both native tryptophans were replaced by phenylalanines; MOPS, 3-(*N*-morpholino)propanesulfonic acid; CD, circular dichroism; UV, ultraviolet; SDS, sodium dodecyl sulfate; PAGE, polyacrylamide gel electrophoresis; Gdn·HCl, guanidine hydrochloride; FWHM, full width at half-maximum.

0006-2960/94/0433-2217$04.50/0

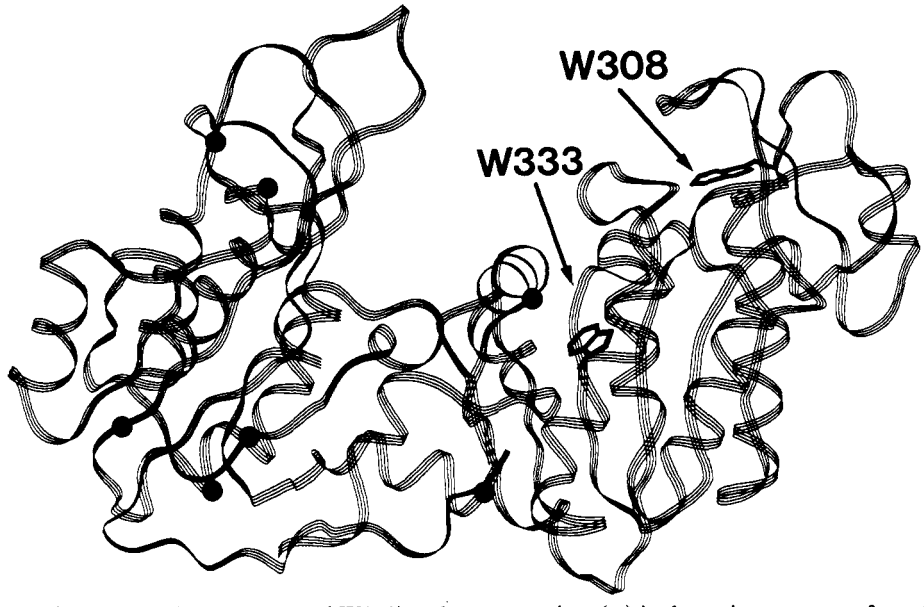

FIGURE 1: Locations of two tryptophans (W308 and W333) and seven tyrosines (●) in the native structure of yeast phosphoglycerate kinase. The ribbon drawing of the PGK structure was made using INSIGHT software (Biosym, San Diego, CA).

suggested that the two longer components were associated with W308 and the major short component with W333. More recently, Dryden and Pain (1989) concluded from steady-state and time-resolved fluorescence quenching studies that both tryptophans have a heterogeneous emission with multiple decay times.

Steady-state fluorescence has been used to monitor the reversible equilibrium unfolding transition of wild-type PGK and the isolated carboxy-terminal domain (Missiakis et al., 1990), using guanidine hydrochloride as a denaturant. The existence of a hyperfluorescent intermediate, not previously reported in earlier folding studies of yeast PGK (Nojima et al., 1977; Adams et al., 1985), was detected by these authors.

The aim of the present study was two-fold: (i) to resolve and characterize the fluorescence properties of the two tryptophans and (ii) to correlate the steady-state and time-resolved fluorescence properties with the structural changes occurring during the equilibrium unfolding process. The long-term goal of this approach is to produce a series of mutants containing single tryptophans situated throughout the structure, designed as local probes of the equilibrium and kinetics of folding of this enzyme. In two of the single-tryptophan mutants described here, W308 PGK and W333 PGK, one of the two native tryptophans has been replaced with a phenylalanine. In the third mutant, both tryptophans have been replaced with phenylalanines to create a no-tryptophan mutant, W⁻ PGK. Far-UV circular dichroism, steady-state fluorescence, and time-resolved fluorescence have been used to monitor the equilibrium unfolding transitions of these mutants and those of wild-type PGK.

EXPERIMENTAL PROCEDURES

Reagents. Guanidine hydrochloride (sequanal grade) was purchased from Pierce. L-Tryptophan was from Aldrich Chemical Co. MOPS was purchased from Sigma and sodium phosphate (monobasic and dibasic) from J. T. Baker. The source of the reagents used in the PGK assay was as reported previously (Mas et al., 1987, 1988).

Production of Single-Tryptophan and No-Tryptophan PGKs. Two single-tryptophan mutants (W308 PGK and W333 PGK) and one no-tryptophan mutant (W⁻ PGK) were constructed by substituting one or both native tryptophans with a phenylalanine. Site-directed mutagenesis experiments, yeast expression, and purification of mutant proteins were performed using previously published procedures (Mas et al., 1986, 1987, 1988).

Determination of Enzyme Activity. Enzyme activity in the direction of formation of 1,3-diphosphoglycerate was measured spectrophotometrically at 25 °C as previously described (Mas et al., 1986), in the presence and absence of 50 mM sodium sulfate.

Determination of Molar Extinction Coefficients. Molar extinction coefficients at 280 nm were determined using the method of Gill and von Hippel (1989). The extinction coefficients at 295 nm were determined from the absorbance spectra of samples at known protein concentrations, on the basis of the extinction coefficients at 280 nm. All spectrophotometric measurements were performed using a Uvikon 860 spectrophotometer (Kontron).

CD Measurements. Circular dichroism measurements were carried out using a Jasco-600 spectropolarimeter and quartz cuvettes of 1-mm path length. Protein solutions (0.05–0.1 mg/mL) were prepared in 20 mM sodium phosphate buffer (pH 7.5). Four scans were recorded for each sample at a scan speed of 20 nm/min and a bandwidth of 1 nm. The scans were then averaged and corrected for the buffer base line. Mean residue ellipticity values, $[\theta]$ (expressed in deg·cm^2 dmol^{-1}), were calculated using a molecular weight of 44 700 for PGK (n = 415 amino acids) (Hitzeman et al., 1982).

Steady-State Fluorescence Measurements. Steady-state fluorescence measurements were performed at 25 °C using a Fluorolog-2 photon counting spectrofluorometer (Spex Industries, Edison, NJ). All measurements were conducted in the ratio mode with 5-nm bandwidths for both the excitation and emission monochromators. Steady-state fluorescence emission spectra were recorded at a scan rate of 1 nm/s. The emission spectra were acquired at an excitation wavelength of 295 nm, in the 300–450-nm range, or at an excitation wavelength of 280 nm in the emission range from 290 to 450 nm. Background fluorescence from buffer and denaturant was also recorded and subtracted from the protein spectra.

Determination of Quantum Yields. Tryptophan quantum yields for WT PGK and single-tryptophan mutants were determined at 25 °C relative to a value of 0.14 for tryptophan

in water (Kirby & Steiner, 1970), using the relationship

$$\frac{Q_{prot}}{Q_{trp}} = \frac{\int I_{prot}}{\int I_{trp}} \frac{A_{trp}}{A_{prot}}$$

where Q is the quantum yield, $\int I$ is the integrated intensity of the corrected emission spectrum over the wavelength range 300–400 nm (excitation, 295 nm), and A is the absorbance at 295 nm (Parker & Rees, 1960). L-Tryptophan and the protein solutions were prepared to have the same optical densities at 295 nm (0.028–0.038 OD range). Quantum yield determinations were performed three times for each protein, and the results were averaged.

Time-Resolved Fluorescence Measurements. Time-resolved fluorescence measurements were performed utilizing a Coherent Antares Nd:YAG laser (Palo Alto, CA), frequency-doubled and synchronously pumping a dual dye jet (Coherent 702) laser using rhodamine 6G and a DODCI saturable absorber. Output pulses from this laser at 295 nm were utilized at 4 MHz and had a pulse width of approximately 1 ps. Time-resolved detection utilized time-correlated single-photon counting with a 6u Hamamatsu (R2809U-01, Bridgewater, NJ) microchannel plate detector, high-frequency 50× amplifiers (Phillips Scientific 774, Mahwah, NJ), constant fraction discriminators (Tennelec 454, Oak Ridge, TN), time-to-amplitude converters (Tennelec 862), and pulse-height analysis analog-to-digital converters (Nucleus PCA-II, Oak Ridge, TN). The instrument response function was approximately 50–80 ps. The collimated fluorescence emission was passed through Glan-Thompson polarizers on automated mounts (ISS, Urbana, IL) and focused onto the entrance slits of a SPEX (Edison, NJ) 0.22-m emission monochromator. A half-wave plate in the excitation beam was utilized to rotate the excitation polarization to horizontal for the determination of the polarization bias (g factor) of the detection instrumentation.

Equilibrium Unfolding Studies. The unfolding transitions for WT PGK and the W308, W333, and W$^-$ mutants were monitored using circular dichroism (CD) and fluorescence (steady-state and time-resolved) techniques. The equilibrium unfolding data were obtained for protein solutions (protein concentration, 0.05–0.1 mg/mL) prepared in 20 mM phosphate buffer (pH 7.5) by monitoring ellipticity at 220 nm and total fluorescence emission intensity (excitation at 295 nm for tryptophan-containing proteins and at 280 nm for the no-tryptophan mutant). The equilibrium unfolding data for WT PGK, W308 PGK, and W333 PGK (protein concentrations, 0.25 mg/mL) in 50 mM MOPS buffer (pH 7.5) in the presence of 100 mM NaCl and varying concentrations of guanidine hydrochloride were obtained by measuring, in parallel, the steady-state fluorescence emission spectra and time-resolved fluorescence and anisotropy decay. A series of protein solutions at identical protein concentrations was incubated in the presence of 0–6 M Gdn·HCl. Protein solutions were incubated for at least 3 h prior to measurement to assure that equilibrium conditions had been reached. The same results were obtained when the incubation time was increased to 24 h. The spectra of buffer solutions were measured for each sample and subtracted from the protein spectra. The unfolding data obtained from steady-state fluorescence spectra were plotted as a function of total emission intensity (area under the emission peak from 310 to 450 nm with excitation at 295 nm or from 290 to 450 nm with excitation at 280 nm), using the InPlot scientific graphics package (GraphPad Software, San Diego, CA). Time-resolved fluorescence data analysis was performed utilizing the Globals Unlimited analysis software (Urbana, IL). The recovered time-resolved fluorescence decay parameters (lifetimes, rotational correlation times, and associated preexponential factors for each component) were plotted as a function of Gdn·HCl concentration using Sigma Plot (Jandel Scientific, Corte Madera, CA) and analyzed as described here.

Analysis of the Unfolding Transitions. The unfolding transitions were analyzed by fitting the experimental data (using a nonlinear least-squares algorithm of Marquardt provided in the Sigma Plot or InPlot software packages) to the equation derived from the denaturant binding model (Aune & Tanford, 1969), as described by Betton et al. (1984) and Missiakis et al. (1990). This method of analysis was selected to allow for a direct comparison of the results with those obtained previously for wild-type yeast PGK by Missiakis et al. (1990).

$$f_U = K_0 C^n / (1 + K_0 C^n) \quad (1)$$

$$K_{app} = K_0 C^n \quad (2)$$

where f_U is the fraction of unfolded protein, C is the denaturant concentration, K_{app} is an apparent equilibrium constant for the unfolding reaction, assuming a two-state model,

$$F \overset{K}{\rightleftarrows} U$$

n is the cooperativity index, and K_0 is a constant. At the transition midpoint (C_m), $f_U = f_F$, $K_{app} = 1$, and

$$1/K_0 = C^n = C_m{}^n \quad (3)$$

Using the above relationships, transition midpoints and cooperativity indexes can be calculated by fitting the observed data to the following equation:

$$Y_{obs} = f_U Y_{max} + (1 - f_U) Y_{min} \quad (4)$$

where

$$f_U = C^n / (C^n + C_m{}^n) \quad (5)$$

The unfolding curves obtained by CD and steady-state fluorescence intensity were normalized to the apparent fraction of the unfolded form, F(U):

$$F(U) = (Y_{obs} - Y_F)/(Y_U - Y_F) \quad (6)$$

where Y_{obs} is the observed total fluorescence emission intensity or ellipticity at 220 nm, determined as described above. The base-line correction was performed for the unfolding curves, whenever necessary, prior to normalization, using linear extrapolation of the base lines in the pre- and posttransition regions to obtain estimates of Y_U and Y_F in the transition region, as described by Pace et al. (1989).

Nonlinear least-squares analyses were performed to obtain free energies ($\Delta G^\circ_{N\text{-}U}$) and slope terms ($m$) using eq 4 of Senear and Bolen (1992).

RESULTS

Characterization of W308 PGK, W333 PGK, and W$^-$ PGK. Mutants in which one or both tryptophans were replaced with phenylalanines were overexpressed in a yeast strain that does not produce wild-type PGK (Sherman et al., 1990). WT PGK was also expressed and purified using the same procedure. Special precautions were taken to obtain the highest possible

Table 1: Specific Activities, Mean Residue Ellipticities, and Molar Extinction Coefficients for WT PGK and the W308, W333, and W⁻ Mutants

	specific activity (units/mg)		mean residue ellipticity (deg·cm² dmol⁻¹)		molar extinction coefficients (M^{-1} cm^{-1})	
	−sulfate	+sulfate	$[\theta]_{208nm}$	$[\theta]_{220nm}$	ϵ_{280nm}	ϵ_{295nm}
WT	450 (100%)	796	−10997	−11504	22797	6660
W333	356 (79%)	676	−11525	−11116	16986	3755
W308	576 (127%)	724	−10717	−10750	16986	4336
W⁻	448 (100%)	579	−9900	−9890	10728	nd

protein purity, in order to minimize a possible contribution of other proteins to the fluorescence properties of PGK and its mutants. Crystallization using ammonium sulfate was introduced as an additional step in the purification procedure for the W⁻ mutant. The purity of the final preparations was estimated to be ≥99%, on the basis of the silver-staining method of protein detection on SDS–PAGE gels.

Enzymatic activities of the purified proteins were measured both in the absence and in the presence of activatory sulfate ions (50 mM). Specific activities, expressed in units/milligram, were calculated using the extinction coefficients listed in Table 1. These molar extinction coefficients, determined by the method of Gill and von Hippel (1989), correspond to the absorbances of 1 mg/mL protein solutions at 280 nm, which are 0.51 for WT PGK, 0.38 for W308 PGK and W333 PGK, and 0.24 for W⁻ PGK. In the absence of sulfate, the specific activities of WT PGK and the W⁻ PGK mutant were virtually identical (Table 1). The specific activity of W333 PGK was decreased by about 21% and that of W308 PGK was increased by 27%, relative to the activity of WT PGK under the same conditions. Considering that 10% differences are commonly observed between different preparations of wild-type PGK, these results suggest that the mutations had a relatively small effect on the enzymatic activity. The specific activity of all four proteins was increased in the presence of 50 mM sulfate, although to different degrees. The extents of activation for the wild-type enzyme (1.8-fold) and for W333 PGK (1.9-fold) are very similar. In contrast, W308 PGK and W⁻ PGK, both of which share the mutation Trp-333 → Phe, exhibit only 1.3-fold activation. In the presence of sulfate, the specific activities of W308 PGK and W333 PGK were slightly lower than the activity of WT (9% and 15%, respectively). The specific activity of W⁻ PGK was decreased by about 27% as compared to WT PGK activity in the presence of sulfate.

In order to evaluate the effects of the mutations on the structure, the far-UV CD spectra were measured for each protein in 20 mM phosphate buffer (pH 7.5) from 190 to 250 nm. The CD spectra of the mutants exhibited two characteristic minima at 208 and 220 nm and were similar to the spectrum of WT PGK. The mean residue ellipticity values at these two wavelengths are given in Table 1. The differences between the spectra of the two single-tryptophan mutants and WT PGK are essentially within experimental error, although they could also be ascribed in part to a change in the tryptophan content (Woody, 1978; Chakrabartty et al., 1993). A slightly larger difference between the ellipticity signal for the W⁻ mutant (10% and 14% decreases at 208 and 220 nm, respectively) could be due to the decreased contribution of aromatic side chains resulting from the substitution of two tryptophans with phenylalanine. It is also possible that small structural changes or an error in the determination of the protein extinction coefficient using the method of Gill and von Hippel (1989), which is based on the absorbance spectra of a set of 30 tryptophan- and tyrosine-containing proteins, might also contribute to this difference.

Fluorescence Emission Spectra of Folded and Unfolded Proteins. (a) Emission Spectra at λ_{ex} = 295 nm. Fluorescence emission spectra (uncorrected) for WT PGK, W⁻PGK, W333 PGK, and W308 PGK in 20 mM phosphate buffer (pH 7.5) in the presence and absence of 4 M Gdn·HCl are shown in Figure 2. The emission maxima determined from these spectra as well as those from the corrected spectra are given in Table 2. Yeast PGK has been known to exhibit unusual fluorescence properties, i.e., a low tryptophan quantum yield in the folded protein followed by a dramatic increase upon unfolding (Nojima et al., 1976, 1977). This has been attributed in part to a possible quenching of tryptophan fluorescence in the native structure. It has been suggested (Wasylewski & Eftink, 1987; Dryden & Pain, 1989) that one of the tryptophans, presumably Trp-308, is quenched by neighboring amino acid residues. It is clear from the spectra of the single-tryptophan mutants shown in Figure 2B,C that the fluorescence emission intensity of both tryptophans increases upon unfolding, indicating that both are quenched in the native state. Under native conditions, the emission maximum in the corrected spectrum of WT PGK is at 332 nm. The emission maximum of Trp-333, a buried residue, is blue-shifted to 314 nm. In contrast, W308, a surface residue, exhibits a 4-nm red shift relative to the WT emission maximum. Upon unfolding, in addition to the significant change in fluorescence intensity described above, there is also a red shift of the emission maxima. A dramatic shift of about 37 nm is observed for W333, whereas WT and W308 emission maxima undergo smaller 19- and 15-nm red shifts, respectively. The fluorescence emission intensity measured for the no-tryptophan mutant is negligible in the tryptophan emission region (Figure 2A). The low emission intensity around 300 nm might be due to a small contribution from the excitation of tyrosine residues at 295 nm (Willis & Szabo, 1989).

(b) Emission Spectra at λ_{ex} = 280 nm. Uncorrected fluorescence emission spectra were measured in 20 mM phosphate buffer (pH 7.5) in the absence and presence of 4 M Gdn·HCl (Figure 3) at a protein concentration of 0.05 mg/mL. The emission spectrum of WT at an excitation wavelength of 280 nm is dominated by tyrosine fluorescence, as reported previously by Nojima et al. (1976). The two single-tryptophan mutants also exhibit a single peak, with the emission maximum at about 307 nm (Figure 3 and Table 2). The W⁻ mutant's spectrum is typical for a protein containing only tyrosine fluorophores and exhibits a single emission maximum at about 304 nm. Upon unfolding, the spectra of WT PGK and the single-tryptophan mutants exhibit two emission peaks, corresponding to the emissions of tyrosine and tryptophan. In contrast, the unfolded W⁻ PGK exhibits a single emission peak with a maximum at the same wavelength as that in the spectrum of the folded protein but with a decreased emission intensity (Figure 3D).

(c) Additivity of Tryptophan Fluorescence Emission in PGK. In order to compare the steady-state emission properties of the two tryptophans in WT PGK with those of the same tryptophans in the single-tryptophan mutants, the emission spectra of WT PGK were compared with the spectra generated by adding the emission spectra of the single-tryptophan mutants and subtracting the spectrum of the tryptophan-less mutant. As shown in Figure 4A,B, the spectra of the sum and WT PGK are virtually identical, both at excitation 280 and 295 nm. The small differences are within the experimental error, due to dilution and background subtraction.

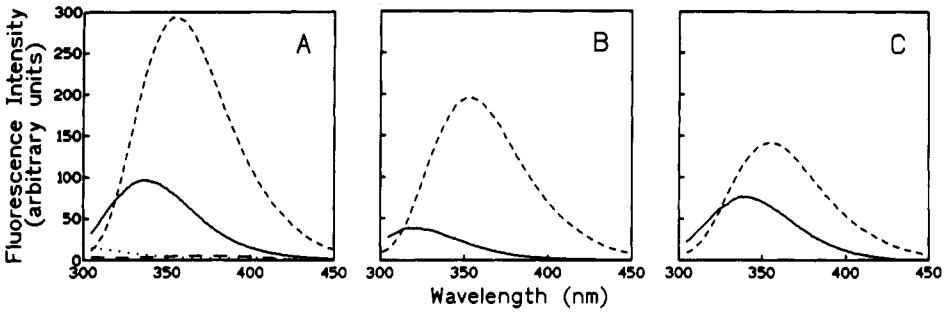

FIGURE 2: Fluorescence emission spectra of wild-type, a no-tryptophan mutant, and two single-tryptophan mutants of phosphoglycerate kinase at excitation wavelength λ = 295 nm in the absence (—) and presence (- - -) of 4 M Gdn·HCl: (A) WT and W⁻ (folded, ···; unfolded, – –); (B) W333; (C) W308. Uncorrected fluorescence emission spectra were recorded using protein solutions (0.1 mg/mL) prepared in 20 mM sodium phosphate buffer (pH 7.5).

Table 2: Fluorescence Emission Maxima and Quantum Yields[a]

	λ_{ex} = 280 nm		λ_{ex} = 295 nm				
			λ_{max} (nm)				
	uncorr λ_{max} (nm)		0 M Gdn·HCl		4 M Gdn·HCl		
protein	0 M Gdn·HCl	4 M Gdn·HCl	uncorr	corr	uncorr	corr	quantum yield
WT	311	~307 353	337	332	355	351	0.03
W333	307	306 352	317	314	356	351	0.02
W308	307	306 351	339	336	355	351	0.038
W⁻	304	304	nd	nd	nd	nd	nd
							Q(W308 + W333)$_{av}$[b] = 0.03

[a] Quantum yields relative to the quantum yield of tryptophan in water (Q = 0.14) were determined as described in the Experimental Procedures. [b] Q(W308 + W333)$_{av}$ is an extinction-weighted average quantum yield.

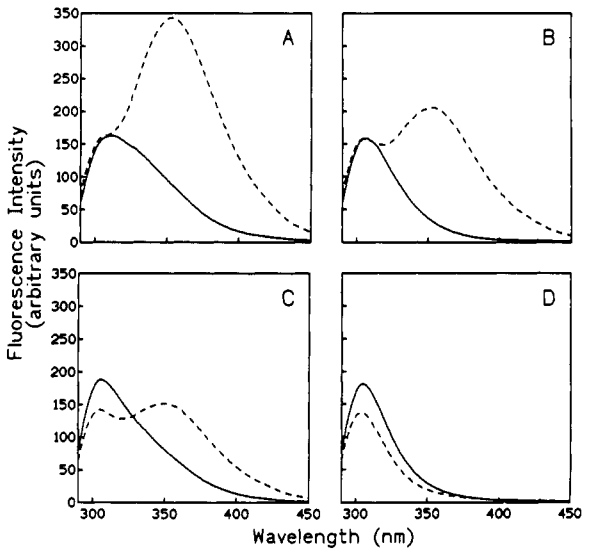

FIGURE 3: Fluorescence emission spectra (uncorrected) of wild-type, a no-tryptophan mutant, and two single-tryptophan mutants of phosphoglycerate kinase at excitation wavelength λ = 280 nm in the absence (—) and presence (- - -) of 4 M Gdn·HCl: (A) WT; (B) W333; (C) W308; (D) W⁻. Protein samples (0.05 mg/mL) were prepared in 20 mM sodium phosphate buffer (pH 7.5).

Tryptophan Quantum Yields in WT PGK, W308 PGK, and W333 PGK. The quantum yields (Table 2) relative to tryptophan in water (Q = 0.14) were determined from the corrected emission spectra at λ_{ex} = 295 nm over the range 300–400 nm, as described in the Experimental Procedures. The quantum yields of W333 and W308 in the single-tryptophan mutants (Q = 0.02 and Q = 0.038) were lower and higher, respectively, relative to the quantum yield of WT tryptophan (Q = 0.03). However, the extinction-weighted

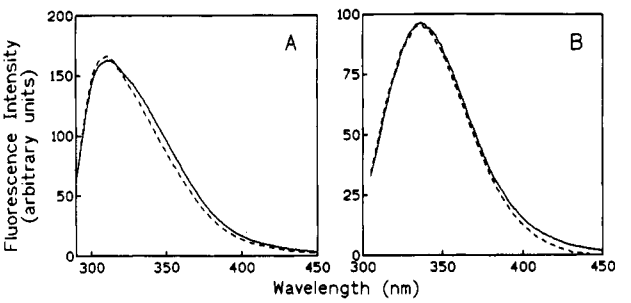

FIGURE 4: Comparison of fluorescence emission spectra of WT PGK (—) and the spectrum generated by adding the emission spectra of the two single-tryptophan mutants and subtracting the spectrum of the no-tryptophan mutant (- - -) (W308 + W333 – W⁻): (A) excitation wavelength λ = 280 nm, protein concentration 0.05 mg/mL; (B) excitation wavelength λ = 295 nm, protein concentration 0.1 mg/mL.

average quantum yield calculated for the sum of W308 and W333, using extinction coefficients given in Table 1, was virtually identical to the quantum yield of the WT protein.

Unfolding Transitions Monitored by CD and Steady-State Fluorescence. Changes in ellipticity at 220 nm as well as changes in total fluorescence emission intensity (Figures 2 and 3D) were utilized to monitor guanidine-induced transitions. The unfolding transitions normalized to the apparent fraction of unfolded protein, F(U), for WT PGK, W308 PGK, W333 PGK, and W⁻ PGK in 20 mM phosphate buffer (pH 7.5) are shown in Figure 5. The protein samples were incubated at each guanidine concentration (from 0 to at least 4 M) for a minimum of 3 h to assure that equilibrium conditions had been reached. The proteins were completely unfolded at 2 M Gdn·HCl, as indicated by the lack of further changes in the monitored optical signals at higher guanidine concentrations. Total fluorescence emission intensity was measured by

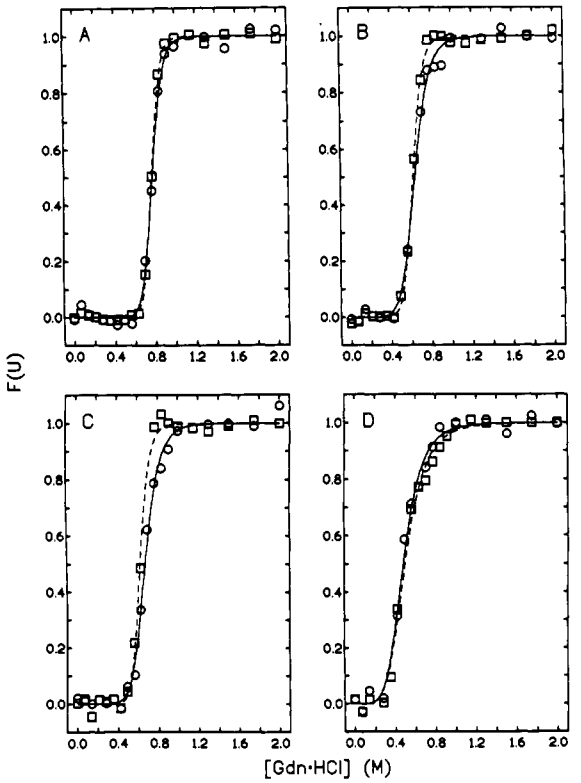

FIGURE 5: Equilibrium unfolding transitions monitored by CD (–O–) and steady-state fluorescence (--□--): (A) WT; (B) W333; (C) W308; (D) W⁻. The fraction of unfolded protein at each Gdn·HCl concentration, calculated from the change in total emission intensity or molar ellipticity at 220 nm, is plotted as a function of the denaturant concentration. All samples were prepared in 20 mM phosphate buffer (pH 7.5). Fluorescence emission spectra were recorded at excitation wavelengths λ = 295 nm (A–C) and λ = 280 nm (D). Solid lines represent the nonlinear least-squares fits to eq 4.

Table 3: Transition Midpoints, Cooperativity Indexes, and Free Energies for the Unfolding Transitions in Phosphate Buffer Monitored by Fluorescence and CD

protein	C_m[a] (M)	n[a]	$\Delta G°_{N\text{-}U}$[b] (kcal/mol)	m[b] (kcal/mol·M)
		Fluorescence		
WT	0.77 (0.76–0.77)	19.8 (18.3–21.3)	11.75 ± 0.35	15.3 ± 0.5
W333	0.62 (0.61–0.62)	13.1 (11.6–14.6)	7.71 ± 0.31	12.5 ± 0.5
W308	0.63 (0.62–0.64)	13.6 (10.5–16.6)	8.04 ± 0.66	12.8 ± 1.1
W⁻	0.49 (0.47–0.51)	4.9 (4.1–5.7)	3.03 ± 0.29	5.9 ± 0.5
		Circular Dichroism		
WT	0.77 (0.76–0.78)	15.7 (12.6–18.8)	9.31 ± 0.71	12.0 ± 0.9
W333	0.63 (0.61–0.65)	9.2 (7.5–10.8)	5.38 ± 0.49	8.4 ± 0.7
W308	0.67 (0.66–0.69)	9.4 (7.8–11.1)	5.68 ± 0.45	8.4 ± 0.7
W⁻	0.48 (0.46–0.50)	5.2 (4.1–6.4)	2.98 ± 0.30	6.1 ± 0.6

[a] Transition midpoints (C_m) and cooperativity indexes were calculated as described in the Experimental Procedures. The 95% confidence intervals are given in parentheses. [b] Free energy changes for unfolding, $\Delta G°_{N\text{-}U}$, were calculated according to eq 4 in Senear and Bolen (1992).

integrating the area under the emission peak at excitation wavelengths λ = 280 nm for W⁻ PGK, which contains seven tyrosines and no tryptophans, and λ = 295 nm for the remaining proteins to excite predominantly tryptophans. The unfolding transitions were corrected for any non-zero base-line slopes, as described by Pace et al. (1989). The transition midpoints and cooperativity indexes (Table 3) were calculated by a nonlinear least-squares fit of the data to eq 4, derived from the model of Aune and Tanford (1969) as described in the Experimental Procedures. This method has been used previously in the analysis of the unfolding transitions of yeast PGK by Missiakis et al. (1990).

As shown in Figure 5A, the unfolding transitions for WT PGK, monitored by CD and fluorescence, are coincident and highly cooperative (Table 3). The fluorescence-detected transition is very symmetrical and differs from the recently reported denaturation curve for WT PGK, which exhibits a characteristic fluorescence maximum at 0.9 M Gdn·HCl (Missiakis et al., 1990). Similar symmetrically shaped unfolding curves were obtained in MOPS buffer (see Table 4 and Figure 6) and when the fluorescence transitions were plotted using fluorescence intensity at a constant emission wavelength, or when the center of mass of the fluorescence emission peak was used (not shown). Increasing the equilibration time to 24 h also failed to produce different results. A curve resembling that reported for WT PGK (Missiakis et al., 1990) was obtained for W308 PGK only once in four unfolding experiments carried out for this mutant in MOPS buffer (data not shown), but was not observed for WT and W333 PGK, although the unfolding experiments for each protein were repeated at least twice in each buffer. It is possible that the discrepancy between our data and the previously published data (Missiakis et al., 1990) might be due to differences in sample preparation.

The unfolding transitions in 20 mM phosphate buffer (pH 7.5) for W333 PGK and W308 PGK, monitored by both CD and fluorescence, are also coincident within experimental error. However, the fluorescence-monitored transitions for the single-tryptophan mutants were more cooperative than their corresponding CD-monitored transitions (Figure 2B,C and Table 3). Coincident transitions were also observed for the W⁻ mutant (Figure 5D). The overall stability of the single-tryptophan mutants is slightly lower than that of WT PGK, as indicated by a decrease in the transition midpoints from 0.77 M Gdn·HCl to 0.63 and 0.67 M for W333 PGK and W308 PGK, respectively (Table 3). The unfolding transitions in 50 mM MOPS buffer (pH 7.5) containing 100 mM NaCl, monitored by changes in total fluorescence emission intensity, also followed a simple two-state unfolding model for all four proteins. The nonlinear least-squares fits and parameters calculated from these data (data points omitted for clarity) are shown in Figure 6 and Table 4, respectively.

Unfolding Transitions Monitored by Time-Resolved Fluorescence Spectroscopy. The time-resolved fluorescence intensity and anisotropy decay data for WT and the two single-tryptophan mutants of PGK, obtained in 50 mM MOPS buffer/100 mM NaCl (pH 7.5), are plotted in Figure 6 as a function of Gdn·HCl concentration (0–2 M). The data in most cases required a minimum of three lifetimes and two rotational terms, as determined utilizing standard statistical criteria (Beechem et al., 1992). Since detailed time-resolved data of this type have not been extensively reported and analyzed, every attempt was made to keep the data analysis as simple as possible, without imposing any particular model concerning how the recovered parameters should change as a function of denaturant concentration. As shown in Figure 6, this simple, unlinked analysis yielded well-defined transitions in the recovered parameters.

It is clear that in all three proteins, the major changes in the time-resolved total intensity parameters are associated with the amplitude factors (α). The predominant amplitude factor is associated with the shortest lifetime and decreases with increasing denaturant concentration. The two amplitudes associated with the medium and long lifetimes reveal a parallel increase as the protein becomes unfolded. Since the lifetime changes observed are relatively small and the data density through the unfolding transition is high, it seems reasonable

Table 4: Transition Midpoints (C_m) and Cooperativity Indexes (n) Calculated from Time-Resolved and Steady-State Data[a]

	protein							
	WT		W308		W333		W⁻	
	C_m (M)	n	C_m (M)	n	C_m (M)	n	C_m (M)	n
α_1	0.72 ± 0.007	18 ± 3	0.64 ± 0.005	14 ± 2	0.54 ± 0.02	11 ± 2		
α_2	0.72 ± 0.009	20 ± 5	0.64 ± 0.007	17 ± 3	0.52 ± 0.02	11 ± 4		
α_3	0.72 ± 0.007	18 ± 2	0.64 ± 0.005	19 ± 1	0.55 ± 0.01	11 ± 2		
τ_1	0.94 ± 0.04	nd	0.52 ± 0.03	11 ± 9	nd	nd		
τ_2	0.61 ± 0.02	15 ± 7	0.69 ± 0.01	16 ± 3	nd	nd		
τ_3	0.54 ± 0.04	nd	0.52 ± 0.01	18 ± 6	nd	nd		
β_1	0.66 ± 0.03	nd	0.53 ± 0.02	28 ± 17	0.67 ± 0.04	8 ± 2		
β_2	0.62 ± 0.03	11 ± 4	0.51 ± 0.07	19 ± 4	0.55 ± 0.02	6 ± 2		
ϕ_1	0.73 ± 0.02	30 ± 22	0.51 ± 0.05	4 ± 2	0.86 ± 0.16	3 ± 2		
T_i	0.71	11	0.6	17	0.55	9	0.45	6

[a] Transition midpoints (C_m) and cooperativity indexes (n) for the unfolding transitions in 50 mM MOPS buffer/100 mM NaCl (pH 7.5) are calculated from the data shown in Figure 6. Time-resolved data are shown in rows 1–9 and steady-state total intensity data (T_i) in row 10. ϕ_1, rotational correlation time for long rotation; β_1, β_2, rotational amplitudes for fast and slow rotation; τ_1, τ_2, τ_3, short, medium, and long lifetimes, respectively; α_1, α_2, α_3, their corresponding amplitudes. Errors in the C_m and n values calculated from the steady-state data (T_i) are within ±2% and ±10%, respectively.

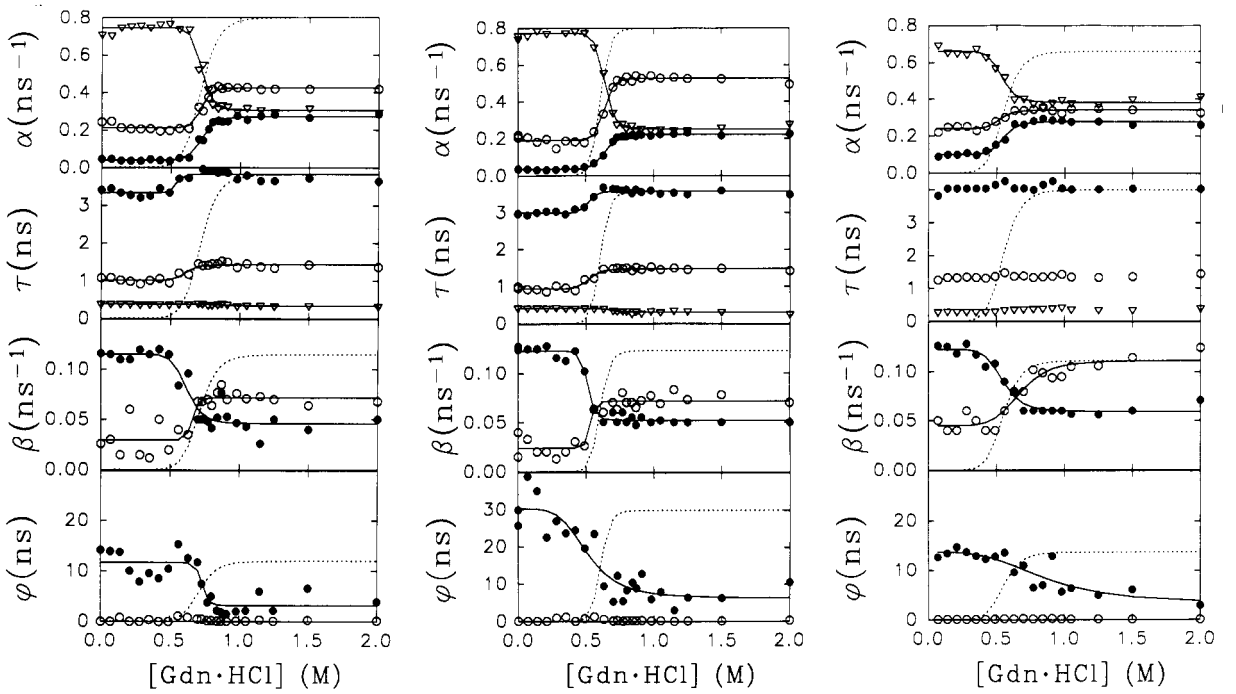

FIGURE 6: Equilibrium unfolding transitions monitored by time-resolved fluorescence: left panel, WT; middle panel, W308; right panel, W333. Population amplitudes (α), lifetimes (τ), rotational amplitudes (β), and rotational correlation times (ϕ) are plotted as a function of Gdn·HCl concentration. Three lifetime terms (short, τ_1; medium, τ_2; long, τ_3) are required to fit the observed total intensity data. In the top two panels these lifetimes and associated amplitudes (α_1, α_2, α_3) are denoted as ▽, ○, and ●, respectively. The amplitude terms are not fractional intensity weighted. Two rotational terms, short (ϕ_1) and long (ϕ_2), are required to fit the anisotropy data. In the bottom two panels the two rotational correlation times and their associated amplitudes (β_1, β_2) are denoted by ○ and ●, respectively. Solid lines represent nonlinear least-squares fits of the observed time-resolved fluorescence data to eq 4. Dashed lines represent nonlinear least-squares fits of a parallel set of steady-state fluorescence (total intensity) data obtained on the same samples (data points omitted for clarity). Transition midpoints and cooperativity index values calculated from these transitions are summarized in Table 4. All experiments were performed in 50 mM MOPS buffer/100 mM NaCl (pH 7.5).

to group together the amplitude terms associated with each lifetime. However, the possibility that a more complicated association between amplitudes and lifetimes exists cannot be ruled out.

Examination of the time-resolved total intensity and anisotropy decays of the folded (0 M guanidine) and unfolded proteins (4 M guanidine) reveals a number of interesting aspects. The normalized total intensity decays in Figure 7 (A–C) were absolutely reproducible (multiple protein preparations and many separate experiments), with W333 always decaying faster initially but having more intensity at later times than either WT or W308. WT decay was always intermediate between W333 and W308, with WT and W308 becoming identical at late times. Both of the native tryptophans are rather severely quenched compared to other tryptophan-containing proteins. For reference, the decay data for another genetically engineered single-tryptophan PGK mutant, with tryptophan at position 194, are included in Figure 7D. This tryptophan yields a more characteristic lifetime (mean lifetime = 4 ns). Upon unfolding, all lifetime differences become very small (Figure 7U).

The anisotropy decays associated with WT, W308, and W333 in the folded form are also distinct. Both WT and W308 have very similar rotational behavior (Figure 7B,C), whereas W333 has a larger decrease in the early anisotropy decay. It should be emphasized that the tryptophan signals for WT, W308, and W333 are not very sensitive to overall Brownian motion due to their very short lifetimes and the

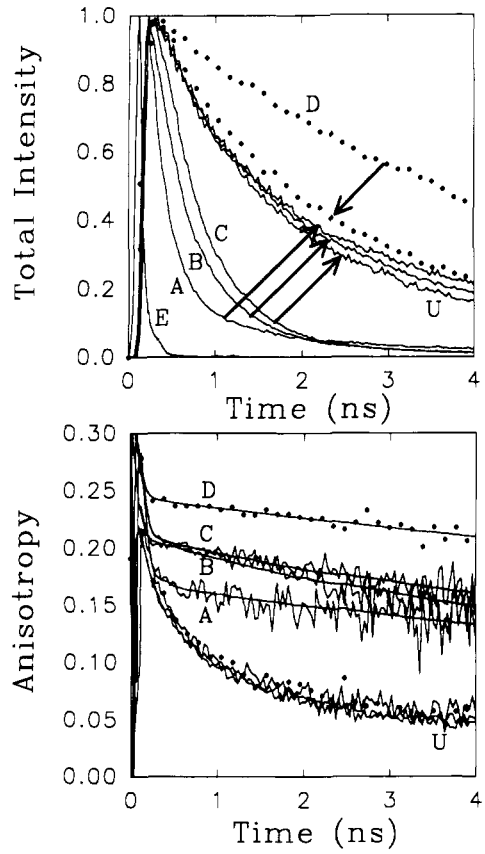

FIGURE 7: Total intensity decay (top) and anisotropy decay (bottom) data for W333 (A), WT (B), and W308 (C) in the absence (A–C) and presence (U) of 4 M Gdn·HCl. Data (every 20th point) obtained for a single tryptophan situated in the interdomain hinge region (W194) are shown for comparison (D). The excitation function (E) shown in the top graph has a FWHM of 60–75 ps.

long predicted correlation time for PGK ($M_r \approx 45\,000$). There does appear to be substantial initial depolarization of all intrinsic tryptophans compared to W194, which appears to be almost completely immobilized. Upon unfolding, all of the observed anisotropy decays become superimposable (Figure 7U). Unfolded states of all of the proteins examined in this study appear to be identical in terms of the time-resolved characteristics.

DISCUSSION

This article describes the characterization of two single-tryptophan mutants of yeast phosphoglycerate kinase and a no-tryptophan mutant, constructed using site-specific mutagenesis. One or both native tryptophans, W333 and W308, have been replaced by phenylalanines to produce W308 PGK, W333 PGK, and W⁻ PGK, respectively. These mutants are the first in a series of single-tryptophan mutants designed to serve as local probes of PGK folding. A comparison of the specific activities CD spectra, and susceptibility to guanidine-induced unfolding indicates that the mutations do not cause significant perturbation of structure or stability relative to WT PGK. Characterization of the steady-state fluorescence properties reveals that both W308 and W333 are quenched in the folded state. The large enhancement of tryptophan fluorescence intensity observed in the presence of denaturant is accompanied by a large red shift of the emission maxima (Figure 2 and Table 2).

Different optical signals are used frequently in protein-folding studies to monitor the structural changes accompanying the unfolding/refolding transition. Ellipticity changes monitored using CD measurements can detect global structural changes. Fluorescence changes reported by native or genetically inserted tryptophans and tyrosines can detect both local and global changes, depending on the folding mechanism and their location in the structure. Both methods were used in the present study to compare the equilibrium unfolding transitions induced by guanidine hydrochloride for WT PGK, W308 PGK, W333 PGK, and W⁻ PGK. The carboxy-terminal location of the two tryptophans in PGK makes them useful for monitoring the unfolding of this domain by selectively exciting tryptophan fluorescence at 295 nm. Tyrosine fluorescence emission was used to monitor the unfolding transition of W⁻ PGK. The tyrosyl residues in yeast PGK are located, with the exception of one C-terminal tyrosine, at a relatively large distance from the two native tryptophans: five in the amino-terminal domain and one in the interdomain region (Figure 1). It is clear that both W308 and W333 reveal transitions identical to those obtained from CD measurements, indicating that no localized unfolding occurs within these two regions of the protein. Symmetrical and coincident transition curves were also obtained by both methods for W⁻ PGK (Figure 5). The unfolding transitions for all four proteins are consistent with a two-state unfolding model.

Both tryptophans exhibit multiexponential fluorescence decay kinetics, with three lifetime components recovered from the analysis of the time-resolved data in the single-tryptophan mutants and WT PGK. The origin of multiple tryptophan lifetimes and amplitude factors in proteins is far from being well-understood (Beechem & Brand, 1985; Lakowicz, 1992). Examination of the time-resolved data for WT PGK and both single-tryptophan mutants, however, reveals a strikingly similar pattern. Despite the large differences in the steady-state properties of buried W333 (blue-shifted 314-nm emission maximum, $Q = 0.02$) and solvent-exposed W308 (336-nm emission maximum, $Q = 0.038$), both mutants have two longer lifetimes and amplitudes that increase with unfolding and a short lifetime and amplitude that decrease with unfolding. A significant question remains as to what physical state these populations represent at each stage of the unfolding transition. One possible interpretation of these data is that the amplitude factors represent the population of different states due to tryptophan rotameric populations, multiple local environments, electron-transfer pathways, or other long-range interactions.

It appears that the data for W308 and W333 do not support local environment effects as being a dominant mechanism that determines the observed time-resolved populations, despite the large difference in the steady-state properties of these mutants. The fact that the emission spectra and quantum yields of the WT enzyme are strictly additive (Figure 4, Table 2) rules out tryptophan–tryptophan energy transfer as a complicating photophysical mechanism. From Figure 2A, it is apparent that the contribution of tyrosine emission using 295-nm excitation and 340-nm emission is minimal and does not add significantly to the observed lifetime heterogeneity.

It thus appears that the short lifetime amplitude term represents a "marker" for the folded state, whereas the other two amplitudes track the unfolded state. A similar pattern has been reported for the guanidine-induced unfolding of staphylococcal nuclease (Eftink & Wasylewski, 1992). Rather remarkably, all three proteins contain distinct lifetime signals which appear to be "markers" for the unfolded state, even in the absence of denaturant. Three possible explanations (among many) are the following: (1) the native state has some lifetime terms which appear in a region very similar to that of the unfolded state; (2) the unfolded lifetime amplitudes

represent a transient small population conformation(s) of the protein with some unfolded characteristics (as sensed by the tryptophan environment); (3) a small amount of denatured protein exists in all sample preparations, although every effort has been made to maintain PGK in the native form. From these experiments it is impossible to determine the exact origin of the "unfolded-like" lifetime populations. Future kinetic experiments are planned that will address these results more directly.

In all cases, the C_m's (Table 3) recovered from the analysis of each amplitude term are virtually identical to those obtained from the steady-state total intensity data. However, in WT and W308 it is clear that the lifetime transitions can precede the main steady-state emission intensity changes (Figure 6, left and middle panels). Since the lifetime changes are relatively small and there are no associated amplitude changes in this pretransition region, the observed steady-state signal change would be very hard to detect. The parallel steady-state fluorescence experiments detected no discernible changes in this region.

The anisotropy parameters represent a more direct measure of overall (and local) protein tertiary structure than do the total intensity parameters. In all three proteins, large shifts in rotational correlation times and their associated preexponential factors occur upon unfolding in the predicted manner. The amplitude term associated with the fast motion component increases with increasing denaturant concentration, whereas the amplitude term that monitors the slower rotation (overall Brownian tumbling) decreases. It does appear that the C_m's for the preexponential associated with the long rotational correlation time also precede the main transition observed with steady-state fluorescence and CD measurements. The uncertainty associated with the C_m's recovered from the rotational correlation times is too great to allow reasonable conclusions to be drawn.

Future equilibrium and kinetic studies of the denaturation and renaturation of several single-tryptophan mutants of PGK should provide further insight both into the mechanism of folding of this two-domain protein and into the physical nature of its fluorescence properties, including their correlation with specific structural changes that occur during the unfolding transitions.

ACKNOWLEDGMENT

We thank Dr. Jerome M. Bailey for performing site-directed mutagenesis experiments. We also thank Drs. David Piston and M. Pilar Lillo for helpful discussions.

REFERENCES

Adams, B., Burgess, R. J., & Pain, R. H. (1985) *Eur. J. Biochem. 152*, 715–720.

Atkins, W. M., Stayton, P. S., & Villafranca, J. J. (1991) *Biochemistry 30*, 3406–3416.

Aune, K. C., & Tanford, C. (1969) *Biochemistry 8*, 4579–4585.

Axelsen, P. H., Bajzer, Z., Prendergast, F. G., Cottam, P. F., & Ho, C. (1991) *Biophys. J. 60*, 650–659.

Beechem, J. M. (1992) *Methods Enzymol. 210*, pp 37–53 and other chapters.

Beechem, J. M., & Brand, L. (1985) *Annu. Rev. Biochem. 54*, 43–71.

Betton, J.-M., Desmadril, M., Mitraki, A., & Yon, Y. M. (1984) *Biochemistry 23*, 6654–6661.

Chakrabartty, A., Kortemme, T., Padmanabhan, S., & Baldwin, R. L. (1993) *Biochemistry 32*, 5560–5565.

Dryden, T. F., & Pain, R. H. (1989) *Biochim. Biophys. Acta 997*, 313–321.

Eftink, M. R., & Wasylewski, Z. (1992) Time-Resolved Laser Spectroscopy in Biochemistry III. *Proc. Int. Soc. Opt. Eng. 1640*, 579–584.

Gill, S. C., & von Hippel, P. H. (1989) *Anal. Biochem. 182*, 319–326.

Harris, D. L., & Hudson, B. S. (1990) *Biochemistry 29*, 5276–5285.

Hitzeman, R. A., Hagie, F. E., Hayflick, J. S., Chen, C. Y., Seeburg, P. H., & Derynck, R. (1982) *Nucleic Acids Res. 10*, 7791–7808.

Kirby, E. P., & Steiner, R. F. (1970) *J. Phys. Chem. 74*, 4480–4490.

Lakowicz, J. R., Ed. (1992) *Topics in Fluorescence Spectroscopy*, Plenum Press, New York.

Loewenthal, R., Sancho, J., & Fersht, A. R. (1991) *Biochemistry 30*, 6775–6779.

Mas, M. T., Chen, C. Y., Hitzeman, R. A., & Riggs, A. D. (1986) *Science 233*, 788–790.

Mas, M. T., Resplandor, Z. E., & Riggs, A. D. (1987) *Biochemistry 26*, 5369–5377.

Mas, M. T., Bailey, J. M., & Resplandor, Z. E. (1988) *Biochemistry 27*, 1168–1172.

Missiakis, D., Betton, J.-M., Minard, P., & Yon, J. M. (1990) *Biochemistry 29*, 8683–8689.

Nojima, H., Ikai, A., & Noda, H. (1976) *Biochim. Biophys. Acta 427*, 20–27.

Nojima, H., Ikai, H., Oshima, T., & Noda, H. (1977) *J. Mol. Biol. 116*, 429–442.

Pace, C. N., Shirley, B. A., & Thomson, J. A. (1989) in *Protein Structure: a practical approach* (Creighton, T. E., Ed.), pp 311–330, IRL Press, Oxford, U.K.

Parker, C. A., & Rees, W. T. (1960) *Analyst 85*, 587–600.

Privat, J.-P., Wahl, P., Auchet, J.-C., & Pain, R. H. (1980) *Biophys. Chem. 11*, 239–248.

Royer, C. A., Gardner, J. A., Beechem, J. M., Brochon, J.-C., & Matthews, K. S. (1990) *Biophys. J. 58*, 363–378.

Senear, D. F., & Bolen, D. W. (1992) *Methods Enzymol. 210*, 463–481.

Sherman, M. A., Szpikowska, B. K., Dean, S. A., Mathiowetz, A. M., McQueen, N. L., & Mas, M. T. (1990) *J. Biol. Chem. 18*, 10659–10665.

Smith, C. J., Clarke, A. R., Chia, W. N., Irons, L. I., Atkinson, T., & Holbrook, J. J. (1991) *Biochemistry 30*, 1028–1036.

Staniforth, R. A., Burston, S. G., Smith, C. J., Jackson, G. S., Badcoe, I. G., Atkinson, T., Holbrook, J., & Clarke, A. R. (1993) *Biochemistry 32*, 3842–3851.

Wasylewski, Z., & Eftink, M. R. (1987) *Eur. J. Biochem. 167*, 513–518.

Watson, H. C., Walker, N. P. C., Shaw, P. J., Bryant, T. N., Wendell, P. L., Fothergill, L. A., Perkins, R. E., Conroy, S. C., Dobson, M., Tuite, M. F., Kingsman, A. J., & Kingsman, S. M. (1982) *EMBO J. 1*, 1635–1640.

Willaert, K., Loewenthal, R., Sancho, J., Froeyen, M., Fersht, A., & Engelborghs, Y. (1992) *Biochemistry 31*, 711–716.

Willis, K. J., & Szabo, A. G. (1989) *Biochemistry 28*, 4902–4908.

Woody, R. W. (1978) *Biopolymers 17*, 1451–1467.